Tractrices, Bicycle Tire Tracks, Hatchet Planimeters, and a 100-year-old Conjecture

Robert Foote, Mark Levi, and Serge Tabachnikov

Abstract. We study a simple model of bicycle motion: A bicycle is a segment of fixed length that can move in the plane so that the velocity of the rear end is always aligned with the segment. The same model describes the hatchet planimeter, a mechanical device for approximate measuring area of plane domains.

The trajectory of the front wheel and the initial position of the bicycle uniquely determine its motion and its terminal position; the monodromy map sending the initial position to the terminal one arises. This circle mapping is a Möbius transformation, a remarkable fact that has various geometrical and dynamical consequences. Möbius transformations belong to one of the three types: elliptic, parabolic, and hyperbolic. We describe a proof of a 100-year-old conjecture: If the front wheel track of a unit bike is an oval with area at least π, then the respective monodromy is hyperbolic.

1. INTRODUCTION. The geometry of the tracks left by a bicycle has received much attention recently [**8, 9, 10, 18, 20, 29**]. In this paper we discuss the connection between the motion of a bicycle and that of a curious device known as a hatchet planimeter, and we will prove a conjecture about this planimeter that was made in 1906.

Bicycle. We use a very simple model of a bicycle as a moving oriented segment in the plane. The segment has fixed length ℓ, the wheelbase of the bicycle. We denote the endpoints of the segment by F and R for the front and rear wheels. The motion is constrained so that the segment is always tangent to the path of the rear wheel. We will refer to this as the "bicycle constraint." This non-holonomic constraint is due to the fact that the rear wheel is fixed on the frame, whereas the front wheel can steer. The configuration space of a segment of fixed length is 3-dimensional (it's the special Euclidean group, topologically, a solid torus), and the bicycle constraint defines a completely non-integrable 2-dimensional distribution on it. This is an example of a contact structure, see, e.g., [**2, 13**]; we shall not dwell on this connection with contact geometry.

If the path of the front wheel F is prescribed, then the rear wheel R follows a constant-distance pursuit curve. The trajectory of the rear wheel is uniquely determined once the initial position of the bicycle is chosen. For example, when F follows a straight line, R describes the classical tractrix; see Figure 1. More generally, one may call the trajectory of the rear wheel R the tractrix of the trajectory of the front wheel F.

On the other hand, if the path of the rear wheel R is given, then the trajectory of the front wheel F is uniquely defined once one fixes the direction of the vector RF, for which there are two choices. The choice is determined by a coorientation of the rear wheel trajectory, that is, by a continuous choice of a normal direction to it. Given a coorientation, the vector RF is determined by the rule that it makes a positive frame with the coorientation. Thus, if the orientation of the segment RF agrees with the orientation of the curve before a cusp, then it disagrees with it after the cusp.

http://dx.doi.org/10.4169/amer.math.monthly.120.03.199
MSC: Primary 70F25, Secondary 53C65

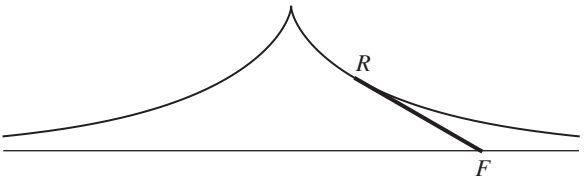

Figure 1. The classical tractrix

One might think that, equally well, one could choose an orientation of the rear wheel track. However, this is not the case: Unlike coorientation, orientation is discontinuous at cusps. Cusps are common for the rear-wheel trajectory; they occur when the steering angle equals 90°, they are where the rear wheel changes its rolling direction. Unless stated otherwise, we assume the trajectory of the front wheel F is smooth.

The study of tractrices goes back to Newton (1676), followed by Huygens, Leibniz, and Euler. To quote from [**4**], "...Euler treated the problem so completely that little or nothing on the subject has appeared since." We hope to make a contribution to this classical subject here.

Prytz Planimeter. The 19th century was a golden age for mechanical innovation. One modest but very useful device was the planimeter, first invented in Bavaria in 1814.[1] A planimeter is an instrument that is used to measure the area of a plane figure by tracing around its boundary. As such, it is a mechanical manifestation of Green's Theorem. There are many types of planimeters, and many improvements have been made over the years, including contributions of Lord Kelvin and James Maxwell. One of the most popular ones was the polar planimeter, introduced in 1854 by Jacob Amsler, a Swiss mathematician and inventor. See [**3, 6, 7, 11, 12, 15, 16, 22, 25**] for a sampler of the vast literature on planimeters.

By comparison, Amsler's planimeter was more accurate, more compact, and easier to use than the earlier instruments, and the older ones quickly became obsolete ([**15**, p. 508]). Nevertheless, to be accurate the planimeter had to be carefully designed and precisely manufactured, and it could be unaffordable for an engineer of modest means. In the late 1800s, Holger Prytz, a Danish cavalry officer and mathematician, devised an economical and simple alternative to Amsler's planimeter [**25, 26**].

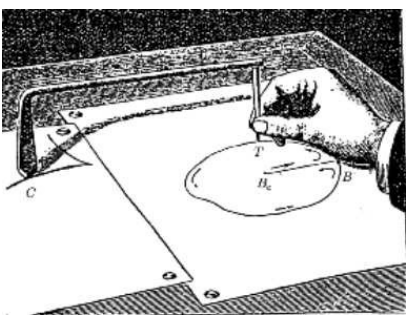

Figure 2. The Prytz Planimeter

Prytz's planimeter consists of a metal rod whose one end, the tracer, is sharpened to a point, while the other end is sharpened to a chisel edge parallel to the rod. (The

[1]The forerunner of the modern bicycle was invented at about the same time, in 1817, by Baron Karl von Drais; the invention was called Draisienne or Laufmaschine.

chisel edge is usually rounded, making it look similar to a hatchet, and consequently the device is also known as a "hatchet planimeter"). It is used by guiding the tracer point along a curve, taking care not to impart any torque. The chisel edge tracks along a curve always tangent to the rod. Thus, the hatchet planimeter satisfies the bicycle constraint, with the chisel edge and tracer point playing the roles of the rear and front wheels, respectively.

It seems unlikely that something as simple (some would say crude) as a hatchet planimeter could measure area. To use it, put the tracer point at some point on the boundary of the region and trace around its boundary. The chisel edge follows a zig-zag path, that is, a path with cusps, similar to the rear wheels of a car when parallel parking; see Figure 3. If the region is small relative to ℓ, the angular deflection of the planimeter is small. When the tracer point returns to the initial position, the chisel edge comes to rest in a slightly different position and makes an angle $\Delta\theta$ with its initial position. The area of the region is $\ell^2\Delta\theta$, at least approximately. There is an inherent error, which actually makes the hatchet planimeter more mathematically interesting than its exact cousins. As we will see, understanding the source of this error can help the user minimize it.

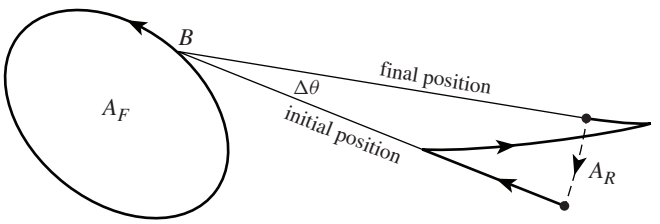

Figure 3. Measuring A_F

Menzin's conjecture. The trajectory of the front wheel of a bicycle determines the trajectory of the rear wheel once the initial position of the bicycle is specified. Given the initial front wheel position, the possible initial rear wheel positions constitute a circle (of radius ℓ). Given a front wheel track, the map $M : \mathbb{S}^1 \to \mathbb{S}^1$ that assigns the terminal position of the bicycle to the initial one is called the *bicycle monodromy*. See Figure 4 for an illustration.

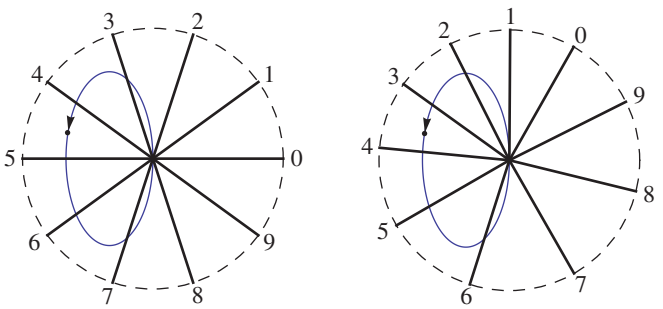

Figure 4. Bicycle monodromy. Left: 10 initial positions of the bicycle; right: the respective 10 positions after traversing the closed path.

If we need to emphasize the dependence of the monodromy of the front track trajectory F, we write M_F. In this paper, the path followed by the front wheel will usually

be closed, so M is a self-map of a circle. The monodromy along a closed path depends on the starting point; another choice of this point results in a conjugated monodromy, i.e., the original monodromy with a change of variables. If the front track trajectory F is not closed, we identify the initial and the terminal circles by a parallel translation; in this way, we think of the monodromy as a circle map for a non-closed path as well. In Section 3 we show that the monodromy is a Möbius transformation (i.e., a fractional linear transformation) acting on the circle of radius ℓ.

For a closed front wheel path, the circle map $M : \mathbb{S}^1 \to \mathbb{S}^1$ has two, qualitatively different, behaviors. If the length of the bicycle ℓ is large compared to the front wheel track, one observes the behavior depicted in Figure 5. In this case, the circle map M is conjugate to a rotation, and it has no fixed points. This is the situation that we encountered when describing the Prytz planimeter. We refer to this behavior as elliptic.

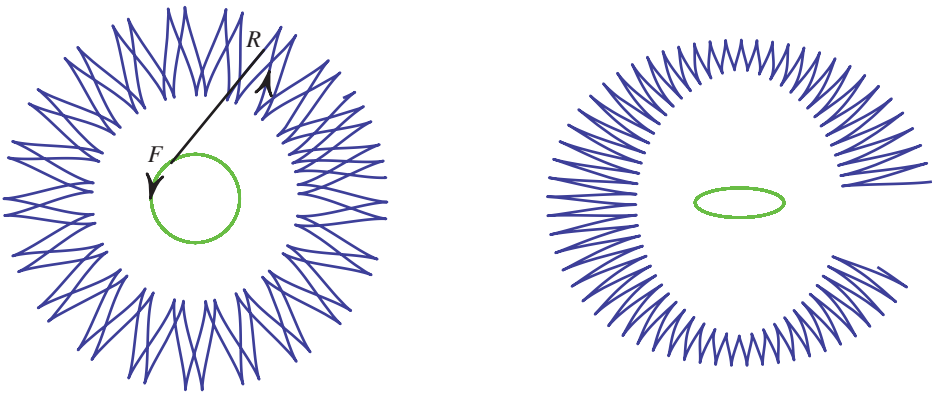

Figure 5. Elliptic monodromy. The front wheel makes multiple passes around the closed curve: Each pass creates one inner and one outer cusp of the rear wheel track.

In contrast, when you ride a bicycle in real life, the distance the front wheel goes is generally much longer than the length of the bicycle (see Figure 9). You don't get bicycle tracks that look like those in Figure 5 unless you are a circus acrobat! When you make a typical round trip on a bicycle, the location of the back wheel at the end of the trip is essentially independent of its initial position; all of the possible rear-wheel trajectories are asymptotic to some particular trajectory in the family, and M has an attracting fixed point; see Figure 6. The map M also has a repelling fixed point—it is

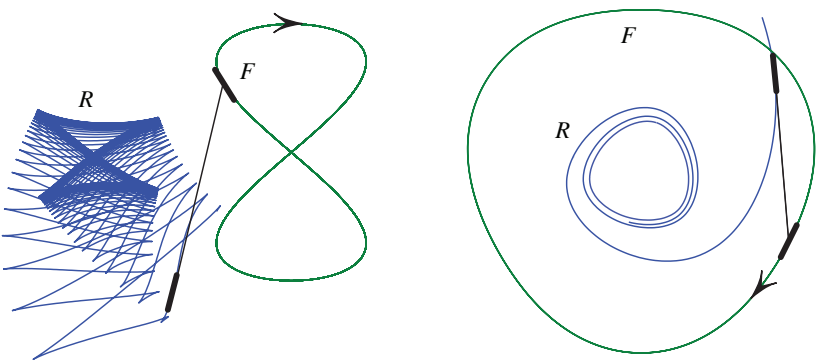

Figure 6. Two examples of hyperbolic monodromy

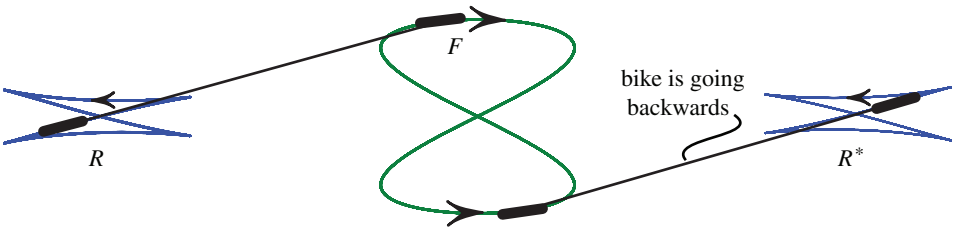

Figure 7. The stable curve is on the left, and the unstable curve on the right. If the direction of traversal of figure eight is reversed, then the two curves exchange stability.

the attracting fixed point when the bicycle runs the route in the opposite direction; see Figure 7. This behavior is referred to as hyperbolic. For animations of this see [**12**]. An intermediate case between elliptic and hyperbolic is the parabolic monodromy: It has one neutral fixed point.

A. L. Menzin was an engineer who invented a slight modification of the hatchet planimeter. More important to us, he made a conjecture in 1906 that explores the boundary between these two different types of bicycle behavior. In his own words [**21**]: "If the average line across the area is long in comparison with the length of the arm, ... the tractrix will approach, asymptotically, a limiting closed curve. From purely empirical observations, it seems that this effect can be obtained so long as the length of arm does not exceed the radius of a circle of area equal to the area of the base curve." In other words, we have the following.

Conjecture 1 (Menzin). *Suppose that the path of F is a simple closed curve bounding a region of area A. If $A > \pi\ell^2$, then M_F has an attracting fixed point.*

For example, if the path of F is a circle of radius $r > \ell$, then the chisel edge will asymptotically approach the circle of radius $\sqrt{r^2 - \ell^2}$ with the same center. This type of behavior is depicted on the right in Figure 6. Similarly, if the path of F is a circle of radius $r = \ell$, then the chisel edge will spiral into the center. There is a qualitative difference between the two cases. If $r > \ell$, then the circle of radius $\sqrt{r^2 - \ell^2}$ is a periodic path attracting nearby trajectories on both sides, but if $r = \ell$, then the center point is attractive only from one side and repelling from the other; see Figure 8. As we explain below, this is the difference between hyperbolic and parabolic dynamical behavior. The situation for $r < \ell$ is shown on the left in Figure 5.

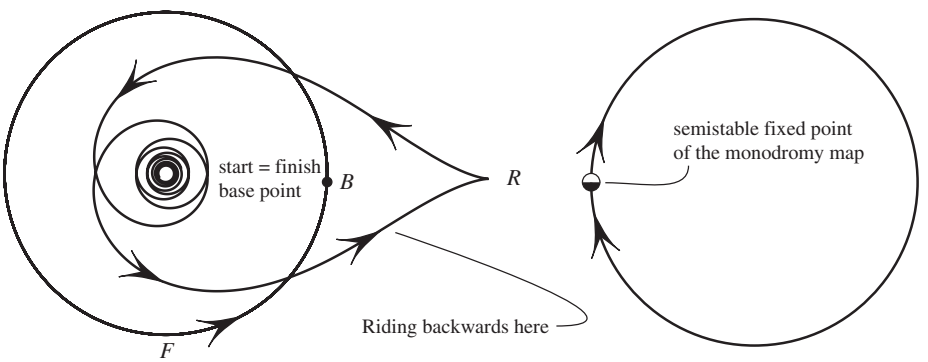

Figure 8. Tractrix of a circle when $r = \ell$. The rear wheel R spirals away from the center while riding backwards; after reversing the direction at the cusp, R spirals into the center. The monodromy is parabolic.

In Section 4, we give a proof of Menzin's Conjecture when the path of F bounds a convex region.

2. THE PRYTZ PLANIMETER AND AREA. To explain how the Prytz planimeter works, let us introduce coordinates (x, y, θ) on the configuration space of segments of length ℓ: The rear end (chisel edge) has coordinates $R = (x, y)$, and the direction of the segment is θ. The front end (tracer point) then has coordinates

$$F = (X, Y) = (x + \ell \cos\theta, y + \ell \sin\theta).$$

The bicycle constraint is the relation $dy/dx = \tan\theta$, or $\lambda = 0$, where

$$\lambda = \cos\theta\, dy - \sin\theta\, dx. \tag{1}$$

Consider an arbitrary motion of the segment such that its initial and terminal positions coincide, that is, consider a loop in the (x, y, θ)-space; this motion may violate the constraint $\lambda = 0$. Denote the signed areas bounded by the closed trajectories of the rear and front ends by A_R and A_F. We are interested in the difference $A_F - A_R$. One has

$$A_R = \frac{1}{2}\int x\, dy - y\, dx \quad \text{and} \quad A_F = \frac{1}{2}\int X\, dY - Y\, dX.$$

A computation yields

$$X\, dY - Y\, dX = (x\, dy - y\, dx) + 2\ell\lambda - \ell\, d(y\cos\theta - x\sin\theta) + \ell^2 d\theta.$$

An exact differential integrates to zero over a closed curve, hence

$$A_F - A_R = \ell \int \lambda + \frac{\ell^2}{2}\int d\theta. \tag{2}$$

The integral $\int \lambda$ measures the net violation of the bicycle constraint. In particular, $\int \lambda$ is the net signed distance that the point R moves in the direction orthogonal to the segment RF. The integral $\int d\theta$ equals 2π times the number of turns made by the segment.

Formula (2) implies that the area under the classical tractrix (Figure 1) is $\pi\ell^2/2$. Indeed, the bicycle constraint is $\lambda = 0$, and the moving segment turns through $180°$.[2] Likewise, the area between the inner and outer tire tracks in Figure 9 is $\pi\ell^2$.

Now consider the hatchet planimeter in its use to measure an area (Figure 3). The tracer point F traverses the boundary of the region being measured, starting and stopping at some base point B, but the chisel edge R does not traverse a closed curve. Close the loop by rotating the segment through an angle $\Delta\theta$ centered at B, which violates the bicycle constraint. We have that $d\theta$ integrates to 0 because the planimeter comes to rest in its original position without making a full rotation. Note that $\lambda = 0$ for the entire motion except the last portion, and we compute that λ integrates to $\ell\Delta\theta$, which is the length of the arc followed by R as it rotates about B through angle $\Delta\theta$. It follows from (2) that $A_F = \ell^2\Delta\theta + A_R$. Provided A_R is small, $A_F \approx \ell^2\Delta\theta$ is a reasonable approximation.

[2]Here we apply a version of (2) involving improper integrals, that is, integration over an infinite curve in the configuration space of segments of length ℓ.

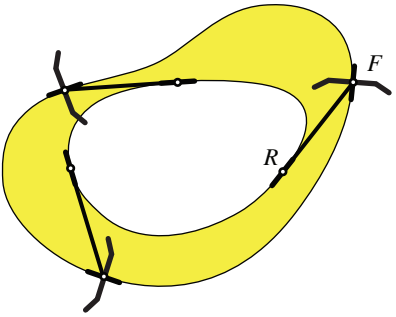

Figure 9. The area between front and rear tracks is $\pi \ell^2$.

How good is the approximation? The error is A_R, the signed area bounded by the zig-zag path of the chisel and the circular arc; see Figure 3. Some starting positions are better than others, as they result in different values of A_R. A suggestion made by most of the authors is to start and stop the tracing at the centroid of the region, as shown in Figure 2. To do this, draw a segment joining the centroid B_c to the base point on the boundary. Start with the tracing point of the planimeter at B_c. Move it along the segment to B, then around the boundary curve back to B, and finally return along the segment to B_c.

Of course, locating the centroid is at least as complicated as computing the area—in practice one simply makes a reasonable guess. Only Prytz [**26**] and Hill [**16**] give enough mathematical details to make this rigorous (see [**11**] for a summary), and their analysis shows that even starting at the centroid does not eliminate the error entirely. They show that, for an arbitrary starting point, the error is $\mathcal{O}(1/\ell)$ and that, starting at the centroid,

$$\ell^2 \Delta\theta = A_F \left(1 + \frac{R^2}{2\ell^2}\right) + \mathcal{O}((d/\ell)^3), \tag{3}$$

where R^2 is the mean-square distance of points in the region from the centroid and d is the diameter of the region. It seems reasonable to conjecture that the full right-hand side of this formula is a weighted sum of all of the even moments of the region.

The history of the Prytz planimeter is one of humor and controversy. Other inventors, misunderstanding the mathematical nature of the error of the device, strove to improve the planimeter by adding scales or wheels that would more accurately measure the arc length $\ell \Delta\theta$ instead of the straight-line distance between the points, defeating the simple, economical design. Prytz scoffed at them, writing [**27**] "rather than use the 'improved [hatchet] planimeters,' let a country blacksmith make them a copy of the original instrument." For more on this amusing history, see [**11, 25**] and their references.

3. BICYCLE MONODROMY.

The monodromy is a Möbius transformation. The Möbius group on $\mathbb{R}$ is the group of orientation-preserving isometries of the hyperbolic plane. A realization of the Möbius group depends on the model of hyperbolic geometry. One model identifies the hyperbolic plane with the upper half plane. The x-axis, complemented with a point at infinity, is the projective line $\mathbb{RP}^1$, the absolute, or the "circle at infinity." The

group of orientation preserving isometries in this model consists of fractional-linear transformations

$$x \mapsto \frac{ax+b}{cx+d} \quad \text{for} \quad a, b, c, d \in \mathbb{R} \quad \text{and} \quad ad - bc > 0.$$

Another model of hyperbolic geometry is the projective (Beltrami–Cayley–Klein) model. The hyperbolic plane is represented by the interior of a disk, the lines are the chords of the disk, the distance is given by the logarithm of cross-ratio (see Figure 10), and the group of isometries consists of the projective transformations of the plane that preserve the disk. In particular, Möbius transformations act on the boundary circle $\mathbb{S}^1$ of the disk. We refer the reader to [**14, 23**] for information about hyperbolic geometry.

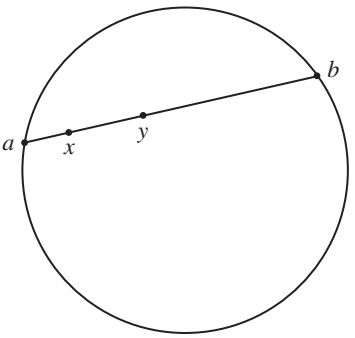

Figure 10. Distance in the projective model: $d(x, y) = \frac{1}{2} \ln \frac{(a-y)(x-b)}{(a-x)(y-b)}$

A stereographic projection identifies the circle $\mathbb{S}^1$ with the projective line $\mathbb{RP}^1$ and conjugates the two actions, by fractional-linear transformations on $\mathbb{RP}^1$, and by projective transformations of the plane on $\mathbb{S}^1$. If ψ is the angular coordinate on the unit circle and $x \in \mathbb{R} \cup \infty$ is the coordinate on the projective line, then the stereographic projection from point $(-1, 0)$ is given by the formula $x = \tan(\psi/2)$.

For example, the following is a 1-parameter group of projective transformations preserving the disk of radius ℓ centered at the origin:

$$f_t : (x, y) \mapsto \frac{\ell}{\ell \cosh t + x \sinh t} \, (x \cosh t + \ell \sinh t, y).$$

Differentiating with respect to t and setting $t = 0$, we find that the infinitesimal generator of this group is the vector field

$$\mathbf{w}(x, y) = \frac{1}{\ell} \, (\ell^2 - x^2, -xy). \tag{4}$$

Readers more familiar with the Poincaré disk model may want to show that the one-parameter group of Möbius transformations

$$g_t(z) = \ell^2 \frac{z + \tanh(t/2)}{\ell^2 + z \tanh(t/2)}$$

on $\mathbb{C}$ preserves the disk of radius ℓ and generates the vector field $(1/\ell)\mathbf{w}$ on its boundary.

The next theorem was proved in [**11**] and extended to arbitrary dimensions in [**20**]. The bicycle monodromy is a self-map of a circle of radius ℓ, which we identify with the circle at infinity in the projective model of hyperbolic geometry.

Theorem 2. *For any front wheel trajectory, the bicycle monodromy is a Möbius transformation.*

Proof. Consider Figure 11. We want to determine the velocity of the rear wheel R relative to the front wheel F. Let $\mathbf{v}$ be the velocity vector of F. Decompose this vector into two components: the one aligned with the segment RF, and the perpendicular component $\mathbf{u}$. If point F moves along the segment RF, then the relative position of R and F does not change. On the other hand, if F moves with velocity $\mathbf{u}$, then R moves, relative to F, with velocity $-\mathbf{u}$.

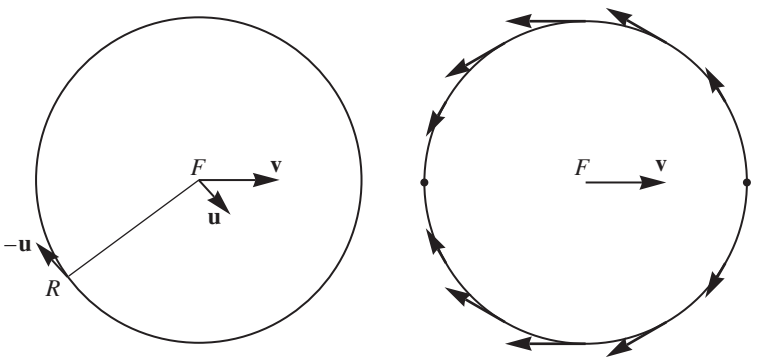

Figure 11. Proof of Theorem 2

Thus, given a vector $\mathbf{v}$, the relative velocity of every point of the circle is the negative of the projection of $\mathbf{v}$ on the tangent line to the circle at this point. We have described a vector field on the circle of radius ℓ, which is an infinitesimal generator of the bicycle monodromy.

To see that this is an infinitesimal Möbius transformation, assume (without loss of generality) that $\mathbf{v} = (1, 0)$. If ψ is the angular coordinate of point R on the circle, then the negative of the projection of $\mathbf{v}$ on the tangent line to the circle at point R is the vector $\sin\psi\ (-\sin\psi, \cos\psi)$. It remains to notice that, for $x = \ell\cos\psi$, $y = \ell\sin\psi$, formula (4) yields the negative of this vector, scaled by ℓ. ∎

Readers familiar with differential geometry may be interested in the following interpretation: The motion of a bicycle defines a parallel translation and connection on the circle bundle over $\mathbb{R}^2$, and Theorem 2 shows that the group for the connection is the Möbius group. For details see [**11**].

A differential equation for the steering angle. Given a trajectory of the front wheel of the bicycle, the bike's position is determined by the steering angle, which we denote by α, as shown in Figure 12. Let t be the arc length parameter along the curve F. The function $\alpha(t)$ is not arbitrary: the bicycle constraint implies a differential equation on it. Let $k(t)$ be the curvature of the front wheel trajectory.

Some versions of the next result appeared in [**1, 8, 10, 20, 29**], and in a different context, in [**5**].

Theorem 3. *One has*

$$\frac{d\alpha}{dt} = k - \frac{\sin\alpha}{\ell}. \tag{5}$$

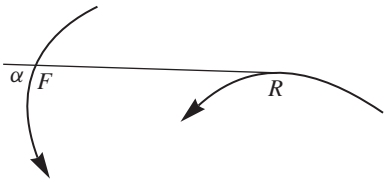

Figure 12. Notation for Theorem 3

Proof. Differentiating $\alpha = \arg F' - \arg RF$ by t and using the definition of curvature, we get $\alpha' = k - \omega_{RF}$, where $\omega_{RF} = \frac{d}{dt} \arg RF$ is the angular velocity of RF. The angular velocity is the same in all frames that do not rotate relative to each other. In the reference frame attached to R and undergoing parallel transport, F moves in a circle of radius ℓ, with speed $v = \sin\alpha$. Thus $\omega_{RF} = v/\ell = (\sin\alpha)/\ell$. ∎

Corollary 3.1. *One has*

$$R' = \frac{\overrightarrow{RF}}{\ell} \cos\alpha.$$

Proof. Since the segment RF has constant length, the speed of R is the projection of the velocity of F on the line RF, i.e., $\cos\alpha$. And the velocity of R aligns with $\overrightarrow{RF}$. ∎

Remark 3.2. In the coordinate $x = \tan(\alpha/2)$ on the projective line, equation (5) becomes a Riccati equation,

$$\frac{dx(t)}{dt} = \frac{1}{2}k(t)(x(t)^2 + 1) - \frac{1}{\ell}x(t).$$

Signed length of the rear wheel track. Real fractional-linear transformations come in three types: elliptic, with no fixed points; parabolic, with one neutral fixed point; and hyperbolic, with two fixed points. For a hyperbolic transformation, one fixed point is attractive and the other repelling. For a parabolic transformation, the fixed point is attractive on one side and repelling on the other, and the eigenvalue at the fixed point is one.

As we mentioned above, the rear track trajectory R may have cusps. The signed length of this curve is the alternating sum of the lengths of its smooth pieces; the sign changes as one traverses a cusp. This signed length is the net roll of the rear wheel of the bicycle. Consider the case when the rear track is a closed curve. Then the bicycle monodromy M of the respective front track is hyperbolic or parabolic. Denote by L the signed length of the rear track.

Theorem 4. *The derivatives of the monodromy at its two fixed points are equal to* $e^{\pm L/\ell}$.

Proof. Let $\alpha(t)$ be a T-periodic solution of the differential equation (5) corresponding to a fixed point of the monodromy. To find the derivative of the monodromy, consider a perturbation $\alpha(t) + \varepsilon\beta(t)$. Substituting into (5) and taking the terms linear in ε yields the linearization

$$\beta'(t) = \frac{\cos\alpha(t)}{\ell}\,\beta(t).$$

This linear equation can be solved as follows:

$$\beta(T) = \beta(0)\, e^{\int \cos\alpha(t)\, dt/\ell}.$$

It follows from Corollary 3.1 that $L = \int_0^T \cos\alpha(t)\ dt$, and so the derivative for this perturbation is $e^{L/\ell}$. The derivative at the other fixed point is then $e^{-L/\ell}$ because the derivatives of a hyperbolic Möbius transformation at its fixed points are reciprocal to each other. ∎

Corollary 3.3. *The monodromy is parabolic if and only if* $L = 0$.

Proof. A hyperbolic Möbius transformation becomes parabolic when its two fixed points merge together and the derivative at this fixed point equals one. ∎

Interpretation of (5): stargazing in H^2. The differential equation (5) describing the bicycle motion has a curious interpretation in terms of hyperbolic geometry. Develop the front track trajectory $F(t)$ in the hyperbolic plane, that is, consider a curve $G(t)$ in H^2 parameterized by the arc length whose curvature is the function $k(t)$. Fix a point A at infinity ("an immobile star"), and let $\alpha(t)$ be the angle made by the geodesic ray $AG(t)$ with the tangent vector $G'(t)$, which we call the stargazing angle, shown in Figure 13.

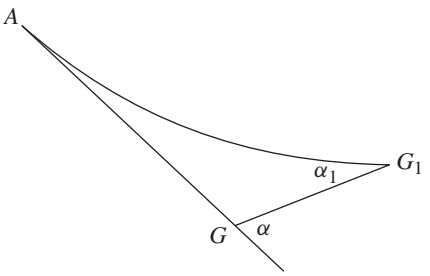

Figure 13. An infinitesimal absolute triangle

Proposition 3.4. *One has* $\alpha' = k - \sin\alpha$.

Thus the equation describing the motion of the unit length bicycle in the Euclidean plane also describes the the retrograde motion of the star due to motion along the curve G in H^2.

Proof. Let G and G_1 be infinitesimally close points on the curve. In the infinitesimally small absolute triangle AGG_1, the angle A is zero and the side $|GG_1| = dt$. The angles of the triangle are $\pi - \alpha$ and $\alpha_1 = \alpha + d\alpha$; see Figure 13. The hyperbolic Cosine Rule (see [**14**]) yields:

$$\cosh(dt)\ \sin\alpha\ \sin(\alpha + d\alpha) = 1 - \cos\alpha\ \cos(\alpha + d\alpha).$$

Expanding both sides to second order and simplifying, we get $d\alpha^2 = \sin^2\alpha\, dt^2$. Then $d\alpha = -\sin\alpha\, dt$, the sign being determined by the fact that $d\alpha/dt < 0$ when $\sin\alpha > 0$.

In addition, the direction of the curve changes from point G to point G_1 by $k(t)dt$, adding this quantity to $d\alpha$. Therefore $\alpha' = k - \sin\alpha$. ∎

We obtain a criterion for the bicycle monodromy to be the identity. Call a differentiable curve C^1-closed if its end points coincide and the oriented tangent lines at the end points coincide as well.

Corollary 3.5. *The development $G \subset H^2$ of the C^1-closed front track F is C^1-closed if and only if the monodromy M_F for the unit length bicycle is the identity.*

Proof. If G is C^1-closed then the stargazing angle $\alpha(t) \mod 2\pi$ is a periodic function for all points A.

Conversely, assume that G is not C^1-closed. Let A_0 and A_1 be its end points, and let L_0 and L_1 be the oriented tangent lines to G at these points. If the monodromy is the identity, then, for each point at infinity X, the lines XA_0 and XA_1 make equal angles with the curve G.

Denote the backward and forward intersection points of L_0 with the circle at infinity by B and C. Then the angles made by the lines BA_0 and CA_0 with G are zero and π respectively, hence the lines BA_1 and CA_1 also make the angles of zero and π with G, and therefore $L_1 = L_0$. It follows that A_1 lies on L_0 and $A_1 \neq A_0$.

Now, let D be the point at infinity such that DA_0 is perpendicular to L_0. Then DA_1 is not perpendicular to L_1 $(= L_0)$, contradicting the assumption that the monodromy is the identity. ∎

For example, let F be a circle of curvature k, traversed p times, and assume that G is a circle of the same curvature, traversed q times. The perimeter length of F is $2\pi p/k$, and that of G is $2\pi q/\sqrt{k^2-1}$ (see [**14**] for formulas of hyperbolic geometry). We obtain the equation

$$\frac{p}{k} = \frac{q}{\sqrt{k^2-1}},$$

hence $k = p/\sqrt{p^2-q^2}$. For example, F can be a circle of radius $\sqrt{3}/2$ (for $p = 2, q = 1$), or radius $3/5$ (for $p = 5, q = 4$).

Corollary 3.6. *If the front track F is a C^1-closed convex curve (traversed once) then the bicycle monodromy M_F is not the identity.*

Proof. Assume first that $\ell = 1$. Let k be the curvature function of F, and assume that its hyperbolic development G is also C^1-closed. Then $\int_F k(t)\,dt = 2\pi$ and, by the Gauss–Bonnet theorem in the hyperbolic plane, $\int_G k(t)\,dt = 2\pi + A$ where A is the area bounded by G. The area bounded by a closed curve with non-negative curvature in the hyperbolic plane is positive. This is a contradiction.

By scaling, the same conclusion is valid for any bicycle length. ∎

4. PROOF OF MENZIN'S CONJECTURE. In this section we prove Menzin's Conjecture 1 in the case when the front wheel track is convex. The property of the monodromy to be hyperbolic (and elliptic, for that matter) is open in the C^1-topology; a small perturbation of the curve does not affect it. Thus, without loss of generality, we assume that F is a smooth strictly convex curve bounding area A.

The plan of the proof is to vary the length of the bicycle, from very small to very large. We show the following.

(1) When ℓ is small, the monodromy is hyperbolic.

(2) When ℓ is large, the monodromy is elliptic.

(3) If ℓ_0 is the smallest length for which the monodromy becomes parabolic, then $A \leq \pi \ell_0^2$.

Since $A > \pi \ell^2$ by assumption, it follows that $\ell < \ell_0$, which is the hyperbolic zone by definition of ℓ_0.

See Figure 14 for a family of closed rear wheel tracks R corresponding to a fixed front wheel track (outer ellipse with arrow) and various bicycle lengths. Note the change of topology of the curve R as the length varies.

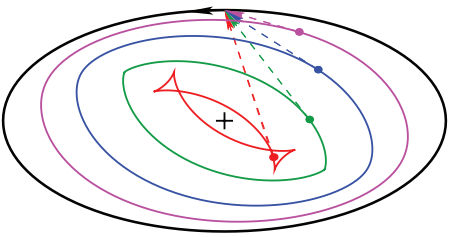

Figure 14. Varying the length of the bicycle (image borrowed from [**19**] with permission)

Let us now proceed to claims (1)–(3).

(1). If ℓ is very small, the monodromy is hyperbolic; this agrees with our experience of riding a bike whose wheel base is much smaller than the length of the path. Here is a more precise sufficient condition for hyperbolicity.

Lemma 4.1. *If $\ell < r$, where r is the radius of the smallest osculating circle to F, then the monodromy M_F is hyperbolic.*

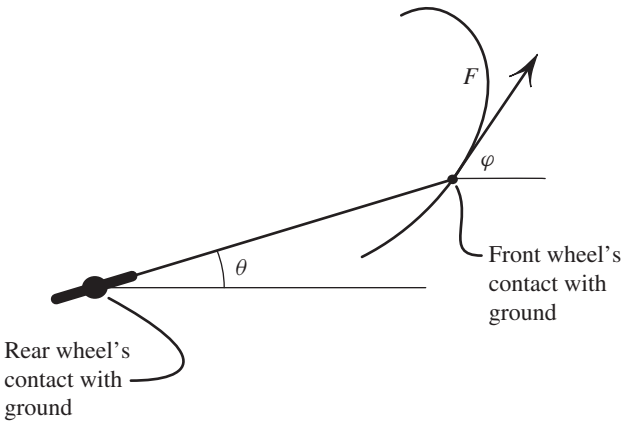

Figure 15. Notations to proof of Lemma 4.1

Proof. In the notations of Figure 15, it follows that

$$\theta' = \ell^{-1} \sin(\varphi - \theta); \tag{6}$$

here $\varphi(t)$ is smooth with $\varphi' \geq 0$ by the convexity of F, since $k(t) = \varphi'(t)$ is the curvature of F. Let $k_{\max} = \max \varphi'(t)$. Then

$$\ell < r = (k_{\max})^{-1}. \tag{7}$$

Consider the strip in the (t, θ)-plane (see Figure 16) given by

$$\varphi(t) - \frac{\pi}{2} \le \theta < \varphi(t) + \frac{\pi}{2}.$$

This strip traps the trajectories of (6); indeed, on the lower boundary $\theta = \varphi - \pi/2$ we have

$$\theta'(t) = \ell^{-1} \sin\left(\varphi - \left(\varphi - \frac{\pi}{2}\right)\right) = \ell^{-1} \overset{(7)}{>} k_{\max} \ge \frac{d}{dt}\left(\varphi(t) - \frac{\pi}{2}\right).$$

A similar condition holds on the upper boundary of the strip, and we conclude that the segment of initial conditions $[\varphi(0) - \pi/2, \varphi(0) + \pi/2]$ maps strictly into its 2π-translate at $t = L$ (the length of F). This implies that the monodromy map $\theta(0) \mapsto \theta(L)$, as a map of the circle, has two fixed points—one inside the arc from $(\varphi(0) - \pi/2, \varphi(0) + \pi/2)$ and another inside a complementary arc. This proves hyperbolicity. ∎

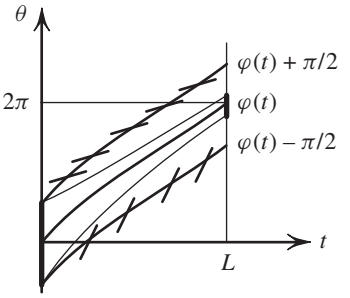

Figure 16. Hyperbolicity for small ℓ

(2). That monodromy is elliptic for sufficiently large ℓ was discussed in Section 2; this is what makes the hatchet planimeter work. To be precise, if F is convex, then $A_F > 0$, and we conclude, according to (3), that if ℓ is large enough, then the turning angle $0 < \Delta\theta < 2\pi$ for all starting points on F and for all starting angles $\theta(0)$. This proves ellipticity. We reiterate that the conjugacy equivalence class of the monodromy does not depend on the starting point (whether it is the centroid of the domain or a point on the boundary).

(3). Now we come to the main part of the argument, the inequality $A \le \pi \ell_0^2$. Let R_0 be the closed rear track corresponding to the bicycle length ℓ_0. We claim that

(i) R_0 has the total rotation of 2π;

(ii) R_0 is locally convex, that is, has no inflection points;

(iii) $A_0 \le 0$, where A_0 is the area A_0 bounded by the curve R_0 given by $\frac{1}{2}\int x\,dy - y\,dx$, as in Section 2.

Item (i) needs an explanation: Even if the curve has cusps, its tangent line is well defined and continuous at all points, and we mean the rotation of this tangent line as one traverses the curve. To prove (i), notice that the total rotation depends continuously on ℓ, and that it is a multiple of 2π for a closed curve. As shown in Step (1), for small ℓ, there is a closed rear wheel curve with total rotation 2π. Thus the total rotation is 2π for R_0 as well.

To prove (ii), assume the opposite. For small ℓ, the rear track is sufficiently close to the front track and hence convex. Thus, non-convexity appears, as ℓ increases, when the curvature of R vanishes and then becomes negative, so that the curve develops a concavity, a "dimple," as shown in Figure 17. This yields a double tangent line L to the curve R, which we orient consistently with the orientation of the rear track R. Then the respective front track F intersects L twice, with the same intersection index (from right to left side in Figure 17). Thus F is not convex, contradicting our assumption.

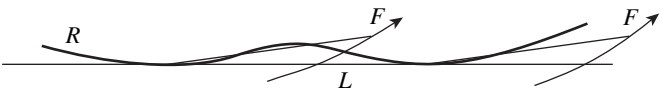

Figure 17. Developing a dimple

To prove (iii), we use the notion of a *support function*. Given a smooth strictly convex closed curve γ, its support function $p(\theta)$ is the (signed) distance from the origin to the tangent line to γ, perpendicular to the direction θ; see Figure 18. The support function determines a 1-parameter family of lines, and the curve γ is recovered as the envelope of this family. The perimeter length of the curve and the area bounded by it are given by the formulas:

$$L(\gamma) = \int_0^{2\pi} p(\theta)\, d\theta, \quad A(\gamma) = \frac{1}{2}\int_0^{2\pi} \left(p^2(\theta) - p'^2(\theta)\right) d\theta, \tag{8}$$

see, e.g., [**28**].

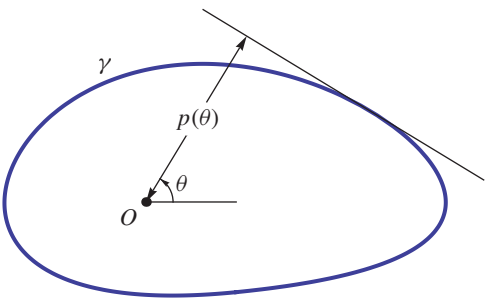

Figure 18. Support function

In fact, support functions can be used to characterize curves that are the envelopes of families of lines parameterized by their direction, that is, 1-parameter families of lines whose direction changes monotonically. As we proved, R_0 is such a curve. Formulas (8) still apply when interpreted as signed length and signed area.

By Corollary 3.3, $L(R_0) = 0$. Thus we claim that

$$\text{if} \quad \int p(\theta)\, d\theta = 0, \quad \text{then} \quad \int p^2(\theta)\, d\theta \le \int p'^2(\theta)\, d\theta.$$

This is the famous Wirtinger inequality, proved by Fourier decomposition of the function $p(\theta)$, see, e.g., [**17**]. This proves (iii).

It remains to relate the areas bounded by the rear and front tracks, that is, A_0 and A. Since the total rotation of the curve R_0 is 2π, formula (2) implies

$$A = A_0 + \pi \ell_0^2 \leq \pi \ell_0^2,$$

as needed. This completes the proof. ∎

5. EXTENSIONS AND RELATED TOPICS. The Menzin Conjecture and its proof were extended to classical geometries of constant curvature ± 1, that is, to the elliptic and the hyperbolic planes [**18**]. These results were obtained as an undergraduate research project in the REU and MASS programs at Penn State.

The bicycle constraint makes sense in both geometries, and the bicycle monodromy is still a Möbius transformation. The spherical and hyperbolic analogs of equation (5) are as follows:

$$\frac{d\alpha}{dt} = k - \cot \ell \ \sin \alpha, \quad \frac{d\alpha}{dt} = k - \coth \ell \ \sin \alpha. \tag{9}$$

Here $\cot \ell$ and $\coth \ell$ are the geodesic curvatures of the circles of radius ℓ in $\mathbb{S}^2$ and H^2, and k is the geodesic curvature of the front wheel track.

Note a curious particular case of (9) in spherical geometry; if $\ell = \pi/2$, then $\cot \ell = 0$, and the bicycle is parallel transported along the front track F. If F bounds area 2π, then the monodromy is the identity (this is a consequence of the Gauss–Bonnet theorem).

Note also the case $\ell = \infty$ in hyperbolic geometry; the second equation in (9) coincides with equation (5) with $\ell = 1$. Since the rear end of an infinitely long bicycle in the hyperbolic plane does not move at all, we recover Proposition 3.4.

An analog of the theorem proved in the previous section is the following result.

Theorem 5. *In $\mathbb{S}^2$: If F is a simple geodesically convex curve bounding area greater than $2\pi(1 - \cos \ell)$, then the monodromy is hyperbolic.*

In H^2: If F is a simple horocyclically convex curve (i.e., having geodesic curvature greater than 1) bounding area greater than $2\pi(\cosh \ell - 1)$, then the monodromy is hyperbolic.

In both cases, the areas are those of the discs of radius ℓ.

We close with the remark that the Wirtinger inequality and the isoperimetric inequality are known to be closely related; see [**17, 24**] for a survey. Additionally, Menzin's conjecture implies the isoperimetric inequality for the front wheel path; see [**11**].

ACKNOWLEDGMENTS. We are grateful to many a mathematician for discussions of "bicycle mathematics." In particular, it is a pleasure to acknowledge interesting discussions with A. Kurnosenko, J. Langer, and R. Perline. M. L. was partially supported by NSF grant DMS-0605878; S. T. was partially supported by Simons Foundation grant No 209361 and by NSF grant DMS-1105442.

REFERENCES

1. J. Alexander, J. Maddocks, On the maneuvering of vehicles, *SIAM J. Appl. Math.* **48** (1988) 38–51, available at http://dx.doi.org/10.1137/0148002.
2. V. Arnold, *Mathematical Methods of Classical Mechanics*. Translated from the 1974 Russian original by K. Vogtmann and A. Weinstein. Corrected reprint of the second (1989) edition. Graduate Texts in Mathematics, 60, Springer-Verlag, New York, 2010.
3. J. Bryant, C. Sangwin, *How Round is Your Circle?* Princeton University Press, Princeton, NJ, 2008.

4. W. Cady, The circular tractrix, *Amer. Math. Monthly* **72** (1965) 1065–1071, available at http://dx.doi.org/10.2307/2315950.
5. A. Calini, T. Ivey, Bäcklund transformations and knots of constant torsion, *J. Knot Theory Ramifications* **7** (1998) 719–746, available at http://dx.doi.org/10.1142/S0218216598000383.
6. C. Care, Illustrating the history of the planimeter, http://empublic.dcs.warwick.ac.uk/projects/planimeterCare2004/Docs/report.pdf.
7. A. Crathorne, The Prytz planimeter, *Amer. Math. Monthly* **15** (1908) 55–57, available at http://dx.doi.org/10.2307/2971268.
8. S. Dunbar, R. Bosman, S. Nooij, The track of a bicycle back tire, *Math. Mag.* **74** (2001) 273–287, available at http://dx.doi.org/10.2307/2691097.
9. D. Finn, Can a bicycle create a unicycle track? *College Math. J.* **33** (2002) 283–292, available at http://dx.doi.org/10.2307/1559048.
10. ———, Which way did you say that bicycle went? *Math. Mag.* **77** (2004) 357–367, available at http://dx.doi.org/10.2307/3219200.
11. R. Foote, Geometry of the Prytz planimeter, *Reports Math. Physics* **42** (1998) 249–271, available at http://dx.doi.org/10.1016/S0034-4877(98)80013-X.
12. ———, Planimeters, http://persweb.wabash.edu/facstaff/footer/Planimeter/Planimeter.htm.
13. H. Geiges, *An Introduction to Contact Topology*, Cambridge University Press, Cambridge, 2008.
14. M. Greenberg, *Euclidean and non-Euclidean Geometries. Development and History*, third edition, W. H. Freeman, New York, 1993.
15. O. Henrici, Report on planimeters, *British Assoc. for the Advancement of Science*, Report of the 64th meeting, 1894, 496–523.
16. F. W. Hill, The hatchet planimeter, *Philosophical Magazine*, S. 5, **38** (1894) 265–269.
17. H. Hopf, *Differential Geometry in the Large*. Lecture Notes in Mathematics, 1000, Springer-Verlag, Berlin, 1983.
18. S. Howe, M. Pancia, V. Zakharevich, Isoperimetric inequalities for wave fronts and a generalization of Menzin's conjecture for bicycle monodromy on surfaces of constant curvature, *Adv. Geom.* **11** (2011) 273–292, available at http://dx.doi.org/10.1515/advgeom.2011.005.
19. A. Kurnosenko. On tractrices of planar curves, arxiv preprint, arXiv:1207.3498.
20. M. Levi, S. Tabachnikov, On bicycle tire tracks geometry, hatchet planimeter, Menzin's conjecture, and oscillation of unicycle tracks, *Experiment. Math.* **18** (2009) 173–186, available at http://dx.doi.org/10.1080/10586458.2009.10128894.
21. A. L. Menzin, The tractigraph, an improved form of hatchet planimeter, *Engineering News* **56** (1906) 131–132.
22. F. J. Murray, *Mathematical machines*, Vol. 2, Analog devices. Columbia University Press, New York, 1961.
23. A. Onishchik, R. Sulanke, *Projective and Cayley-Klein Geometries*, Springer-Verlag, Berlin, 2006.
24. R. Osserman, The isoperimetric inequality, *Bull. Amer. Math. Soc.* **84** (1978) 1182–1238, available at http://dx.doi.org/10.1090/S0002-9904-1978-14553-4.
25. O. Pedersen, The Prytz planimeter, in *From Ancient Omens to Statistical Mechanics*, Edited by J. Berggren and B. Goldstein, University Library, Copenhagen, 1987, 259–270.
26. H. Prytz (pseudonym 'Z'), Stangplanimetret, *Den Tekniske Forenings Tidsskrift* **10** (1886) 23–28.
27. ———, The Prytz Planimeter (two letters to the editor), *Engineering*, September 11, 1896, p. 347.
28. L. Santalo, *Integral Geometry and Geometric Probability*, Cambridge University Press, Cambridge, 2004.
29. S. Tabachnikov, Tire track geometry: variations on a theme, *Israel J. Math.* **151** (2006) 1–28, available at http://dx.doi.org/10.1007/BF02777353.

ROBERT FOOTE received his B.A. from Kalamazoo College in 1976 and his Ph.D. from the University of Michigan in 1983. In addition to mathematics and teaching, he enjoys bicycling and woodturning, examples of which can be seen by googling S^1*-Actions in Wood.*
Department of Mathematics, Wabash College, Crawfordsville, IN 47933
Footer@wabash.edu

MARK LEVI is a professor in the Department of Mathematics at the Pennsylvania State University. He received his Ph.D. from the Courant Institute under the direction of Jürgen Moser. His research interests include differential equations and dynamical systems with applications to physical problems. One of his hobbies is creating and collecting physical devices that he uses to illustrate mathematical phenomena. This collection includes a 7-foot cycloidal trough used to demonstrate three remarkable properties of the cycloid discovered

by Huygens over three hundred years ago. His other hobby is inventing and collecting physical puzzles, some of which can be seen on his website or in his recent book.
Department of Mathematics, Penn State, University Park, PA 16802
levi@math.psu.edu

SERGE TABACHNIKOV received his Ph.D. from Moscow State University in 1987. Since 1990, he has been a professor of mathematics in the US. His research interests include geometry, topology, and dynamical systems. In the late 1980s, he headed the Mathematics Section of Kvant (Quantum), a Russian magazine on physics and mathematics for high school and college students, somewhat akin to the MONTHLY. He is currently the Director of the Mathematics Advanced Study Semesters (MASS) program at Penn State.
Department of Mathematics, Penn State, University Park, PA 16802
tabachni@math.psu.edu

A lecture by Wendelin Werner, a visit to the Town Musicians in downtown Bremen, and the summer school participants during a plenary lecture.